

22 cases. Theoretical models are discussed to elucidate co-precipitation behaviors under various pH
23 scenarios. Notably, ferric chloride coagulation increased the UV absorbance of treated leachate
24 significantly by up to 10 times, while aluminum sulphate only slightly decreased it. It is
25 exacerbated by the complexes formed by ferric and organic matter, which have characteristic light
26 absorption in the UV range. The formation of such complexes is supported by the Fourier
27 Transform Infra-Red (FTIR) spectroscopy. In addition, the volatile acids in leachate were found
28 to play an important role in mediating pH through their buffering capacity.

29

30 **Keywords:** Landfill leachate; Chemically Enhanced Primary Treatment; UV Quenching
31 Phenomenon; Dissolved Organic Carbon; Metal Complexation.

32

33 **1. INTRODUCTION**

34 In the USA, 50-60% of the municipal solid waste (MSW) is disposed of in landfills as it is the
35 most economical and convenient method based on an US EPA survey (US EPA, 2017). In landfills,
36 a large volume of leachate is generated continuously. Based on a survey by the Environmental
37 Research and Education Foundation (EREF), approximately 27 billion liters of leachate was
38 generated in 2017 in the U.S. (Bolyard, 2017). More than 60% of the landfill leachate is discharged
39 to Publicly Owned Treatment Works (POTWs) in the U.S. as it is convenient and cost-effective
40 (Aarts, 1994; Bolyard, 2017; Karidis, 2016). In a landfill, the cost of leachate management
41 contributes the highest portion among all operation and maintenance. Hence, co-treatment with
42 sewage in POTWs is the most common practice for leachate disposal (Zhao et al., 2013a).

43 Over the recent decade, POTWs have been switching from chlorination to other disinfection
44 alternatives because chlorine disinfection has been found to produce secondary contamination due
45 to production of Disinfectant By-Products (DBPs). UV disinfection is a promising method because
46 it is highly effective, DBP free, chemical free, etc. However, landfill leachate that contains a high
47 concentration of organic matter can interfere with the UV disinfection process, as the recalcitrant
48 organic matter can strongly absorb the UV light (Iskander et al., 2018; Zhao et al., 2013b). Even
49 after upfront biological treatment, the residual recalcitrant organic matter further interferes with
50 the downstream UV disinfection in POTWs (Gupta et al., 2014a). Hence, POTWs are prudential
51 on accepting landfill leachate (Karidis, 2016). In wastewater treatment practices, POTWs
52 operating with a UV disinfection unit typically requires 60 – 65% transmittance at 254 nm
53 wavelength to achieve the appropriate level of disinfection (Basu et al., 2007).

54 Chemically Enhanced Primary Treatment (CEPT) is a chemical treatment used in POTWs to
55 enhance the removal of suspended solids, organic matter, and nutrients (such as phosphorus). In
56 the CEPT process, chemical coagulants are typically added to the primary sedimentation basin.
57 CEPT can help reduce the solids and organic loading rate on biological treatment, the treatment
58 infrastructure requirement and overall capital cost (Chagnon and Harleman, 2005). CEPT process
59 is also considered to be a cost-effective method for wastewater treatment in developing countries
60 (Harleman and Murcott, 1999), as it is advantageous in saving footprint (Aiyuk et al., 2004), has
61 low energy requirement (De Feo et al., 2008), and is easy to operate and maintain (Jordão and
62 Volschan, 2004). The efficiency of CEPT in a primary treatment facility depends on the type and
63 dose of coagulant, pH level, temperature and alkalinity (Jiang, 2015). Hence, CEPT, which is
64 coagulation-flocculation in essence, can potentially remove the recalcitrant organic matter carried
65 by landfill leachate and potentially have beneficial impacts on the UV disinfection during sewage-

66 leachate co-treatment in POTWs. However, it has also been found that coagulant with metal salts
67 can increase the UV absorbance due to the interaction between metal cations and organic matter
68 or macromolecules such as humic acid. Such phenomenon has been reported in previous studies
69 where interaction between ferric ion and organic macromolecules increases the UV absorbance
70 (Doane and Horwáth, 2010; Maloney et al., 2005).

71 In this experimental study, the overall goal is to mimic the scenario that sewage and landfill
72 leachate are co-treated in a POTW using CEPT methods in order to evaluate the overall treatment
73 efficacy and beneficial effects of CEPT for the co-treatment, especially the effects on the UV
74 quenching phenomenon. The objectives are: (a) to evaluate the overall organic matter removal
75 performance of CEPT in co-treatment of landfill leachate and sewage; (b) to reveal the
76 exacerbating effect of UV quenching by CEPT; and (c) to provide theoretical explanations for the
77 effects of CEPT on UV quenching.

78

79 **2. MATERIALS AND METHODS**

80 **2.1 Leachate Sample**

81 Leachate samples were collected from landfill sites A and B in Virginia and Ohio, respectively. In
82 each landfill site, leachate samples were collected from two different zones, denoted as normal
83 leachate and concentrated leachate, respectively. Table 1 shows the characteristics of the raw
84 leachate collected from the two different zones in each site. It was observed that the normal
85 leachate and concentrated leachate are very different in terms of physical, chemical and
86 biochemical characteristics. The normal leachate samples from both sites shared slightly alkaline
87 pH, lower organic component concentrations, higher specific ultraviolet absorbance (SUVA) and

88 lower iron, while both the concentrated leachate samples shared acidic pH, higher organic
 89 component concentrations, lower SUVA and higher iron.

90 **Table 1: Characteristics of Raw Leachate Samples**

<u>Parameters</u>	Site A		Site B	
	Normal	Concentrated	Normal	Concentrated
pH	7.8	5.5	8.6	5.4
Iron (mg/L)	2 ± 0.79*	840 ± 18	40 ± 9	800 ± 21
COD (mg/L)	18,000 ± 165	90,000 ± 393	17,870 ± 186	100,000 ± 387
TOC (mg/L)	4,000 ± 32	30,000 ± 149	3,380 ± 57	33,000 ± 201
UV Absorbance (cm⁻¹)	41 ± 3	280 ± 15	120 ± 8	250 ± 12
Volatile Acids (as mg/L CH₃COOH)	785 ± 10.45	22,850 ± 10.34	1,628 ± 44.28	27,700 ± 588
SUVA (L/mg·m)	1.025	0.933	3.550	0.758

91 *: ± is standard deviation.

92

93 Leachate samples were collected in 5-gallon sealed opaque buckets, transported, and stored at 4 °C
 94 before further testing and analysis.

95 **2.2 Coagulants**

96 Ferric chloride (BeanTown Chemical, Hudson, NH, USA) and aluminum sulphate (VWR
 97 International, Radnor, PA, USA) were used as coagulants. Ferric Chloride and Aluminum Sulphate
 98 were chosen as coagulants as they are industrially accepted and widely applied in water and
 99 wastewater treatment in primary treatment. Stock solutions of the coagulants were prepared and
 100 stored at 4 °C for experimental use. The concentration of prepared stock solutions of ferric chloride
 101 and aluminum sulphate was 10 g/L. Application of stock solution is preferred compared to adding
 102 solid coagulant for testing, since the dissolved coagulants can mix rapidly compared to the solid

103 coagulant. For every coagulation experiment, fresh stock solutions were prepared on weekly basis
104 for quality control.

105 **2.3 Experimental Setup**

106 Jar test experiments were set up to replicate CEPT treatment. Experiments were carried out using
107 a Velp flocculator jar testers with six paddles (Cole-Parmer, Vernon Hills, IL, USA) that comply
108 with ASTM D2035 (Bridgewater et al., 2012). Samples were prepared by mixing 5% leachate and
109 95% sewage to mimic the blending of sewage and landfill leachate in POTWs. Then coagulation-
110 flocculation tests were performed on these samples. Prior to running any jar test, samples were
111 brought to room temperature and filtered through 0.45 μm filter paper. The 10 g/L of stock
112 solutions for each coagulant was used to add the coagulants to each jar with different doses. For
113 this study, no fixed coagulant range was predetermined as the normal leachate and concentrated
114 leachate had significantly different organic matter concentration levels. Hence, in this study, the
115 coagulant dose was added in increments of 200 mg/L using the 10 g/L stock solution, until a
116 plateau trend was observed in the organic matter removal, indicating a maximum percentage
117 removal achievable. As per the Standard Method ASTM D 2035 (Bridgewater et al., 2012), 1
118 minute of rapid mixing at 100 rpm and 30 minutes of slow mixing at 25 rpm was performed after
119 the addition of coagulant stock solution to each jar at different doses. After the mixing, 30 minutes
120 was considered for settlement of precipitates. The supernatants from the jar test were collected
121 after filtering through 0.45 μm filter paper to remove precipitates completely. The filtered
122 supernatants were collected and stored at 4 °C for further analysis.

123 The same coagulation-flocculation experiments were conducted for a mixture of 5% leachate and
124 95% de-Ionized water for (a) to compare the result with co-treatment of landfill leachate and
125 sewage, and (b) to determine whether sewage has a different effect on the treatment than water.

126 De-ionized water was collected from a benchtop Milli-Q water purification system
127 (MilliporeSigma, Burlington, MA, USA) for the experiments. The results for the experiments for
128 5% leachate and 95% de-ionized water have been shown in the supporting documents for reference.

129 **2.4 Chemical Analysis**

130 All the tests were carried out by following standard methods provided by American Public Health
131 Association (APHA)(Bridgewater et al., 2012). All the glassware used in the analysis were cleaned,
132 rinsed and dried before usage for quality control purpose.

133 The collected supernatants were analyzed for pH, Chemical Oxygen Demand (COD), volatile
134 acids, Total Organic Carbon (TOC), residual iron and aluminum concentration, UV absorbance,
135 and characterized with Fourier-Transformed Infrared analysis (FTIR). COD was tested using DR
136 6000 spectrophotometer (HACH, Loveland, CO, USA) with HACH ultra-high range TNT823
137 (250-15000 mg/L) and high range TNT822 (20-1500 mg/L). TNT872 test kit ((HACH, Loveland,
138 CO, USA) was used for the volatile acid. TNTplus 858 (HACH, Loveland, CO, USA) was used
139 for iron (Fe) with 1,10-phenanthroline method (ASTM E394, (Bridgewater et al., 2012)). TNTplus
140 848 (HACH, Loveland CO, USA) was used for aluminum (Al) with Chromazurol S method. pH
141 value was tested with an Intellical PHC281 water quality laboratory refillable pH electrode (HACH,
142 Loveland, CO, USA). TOC was tested using TOC analyzer (Teledyne Tekmar, Mason, OH, USA)
143 with three trials for each sample to obtain accurate results and were averaged to measure the
144 standard deviation for accuracy checks and quality control.

145 The UV absorbance of the supernatant was measured at 254 nm using HACH DR6000
146 spectrophotometer with a 1 cm wide quartz cuvette. One key factor for UV spectroscopy was
147 filtering the supernatant by 0.45 μm filter paper to avoid any error in UV absorbance testing due

148 to solids in the supernatant, as suspended and colloidal solids can scatter the light and cause the
149 change in the value of UV absorbance.

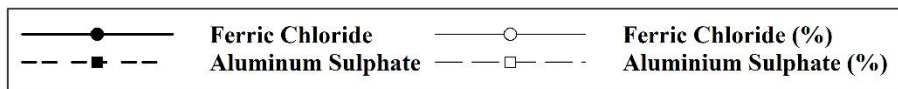
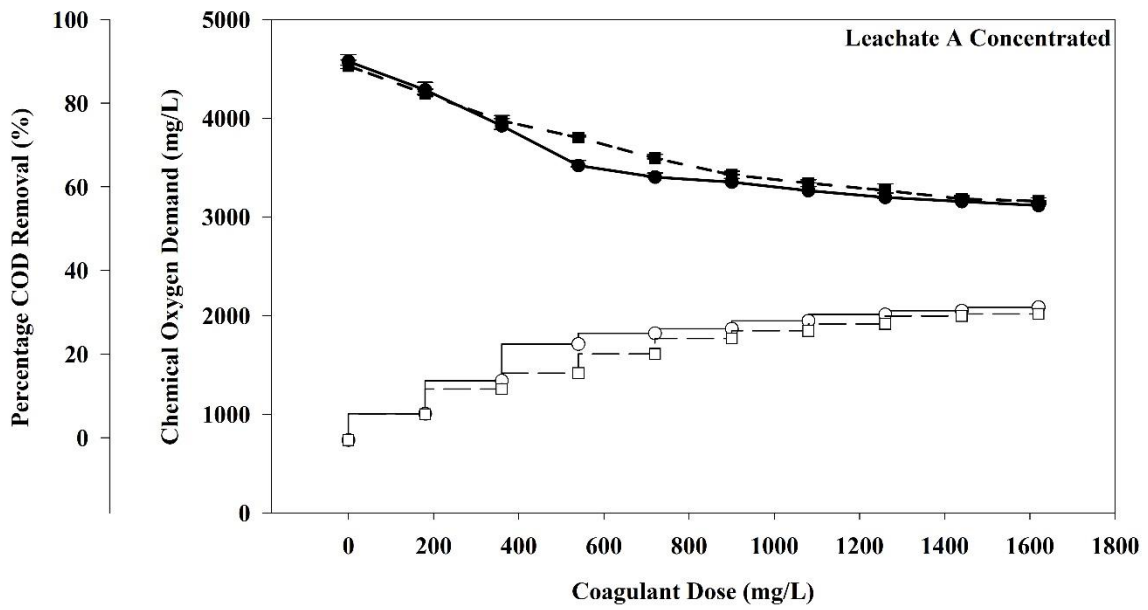
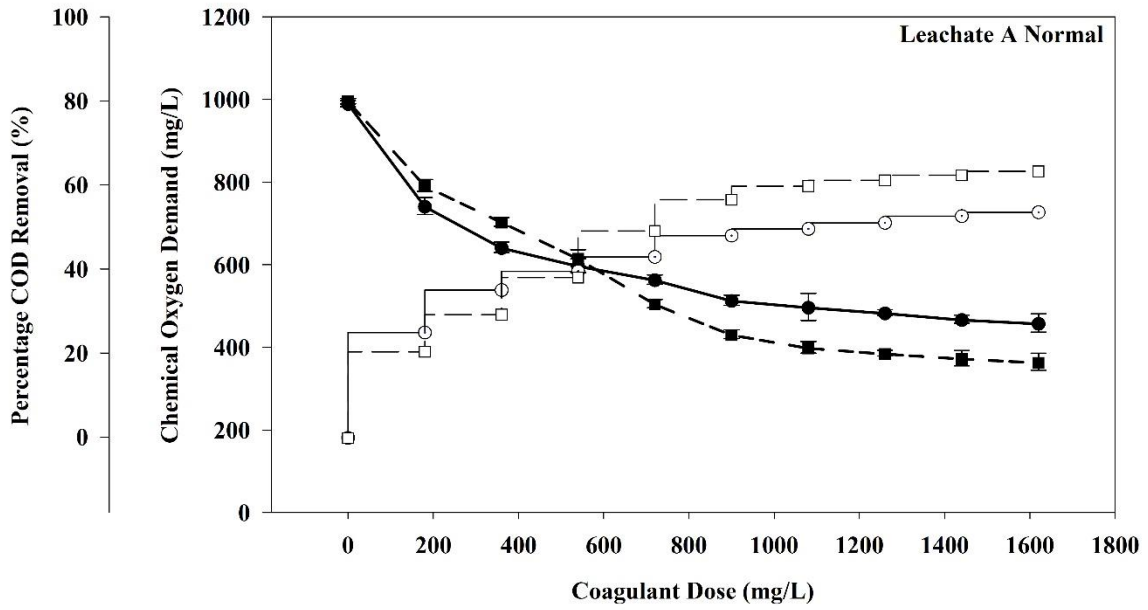
150 Samples for FT-IR spectroscopy were prepared by freeze-drying the supernatants and preparing
151 KCl pellet with a hydraulic press. 20 mL of each supernatant was freeze-dried using FreeZone
152 Legacy freeze dryers (Labconco Corporation, Kansas City, MO, USA) as the moisture in the
153 sample can interfere with FTIR spectra. Nicolet iS50 FTIR spectrophotometer (Thermo Fisher
154 Scientific, Waltham, MA, USA) was used for generating FT-IR spectra provided in the results.

155

156 **3. RESULTS AND DISCUSSION**

157 **3.1 Organic Matter removal**

158 Figure 1 shows the COD removal for normal and concentrated leachate samples from sites A and
159 B by ferric chloride and aluminum sulphate, respectively. Figure 1(a) is for site A. As shown in
160 Figure 1(a), the COD concentration of site A normal leachate was decreased from 990 mg/L to
161 459 mg/L and 365 mg/L by ferric chloride and aluminum sulphate, respectively. And the COD
162 concentration of site A concentrated leachate decreased from 4,592 mg/L to 3,136 mg/L and 3,178
163 mg/L by ferric chloride and aluminum sulphate, respectively. Maximum COD removals of 63.35%
164 and 31.71% were achieved by coagulation for site A normal and concentrated leachates,
165 respectively.



166

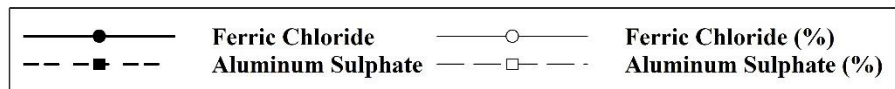
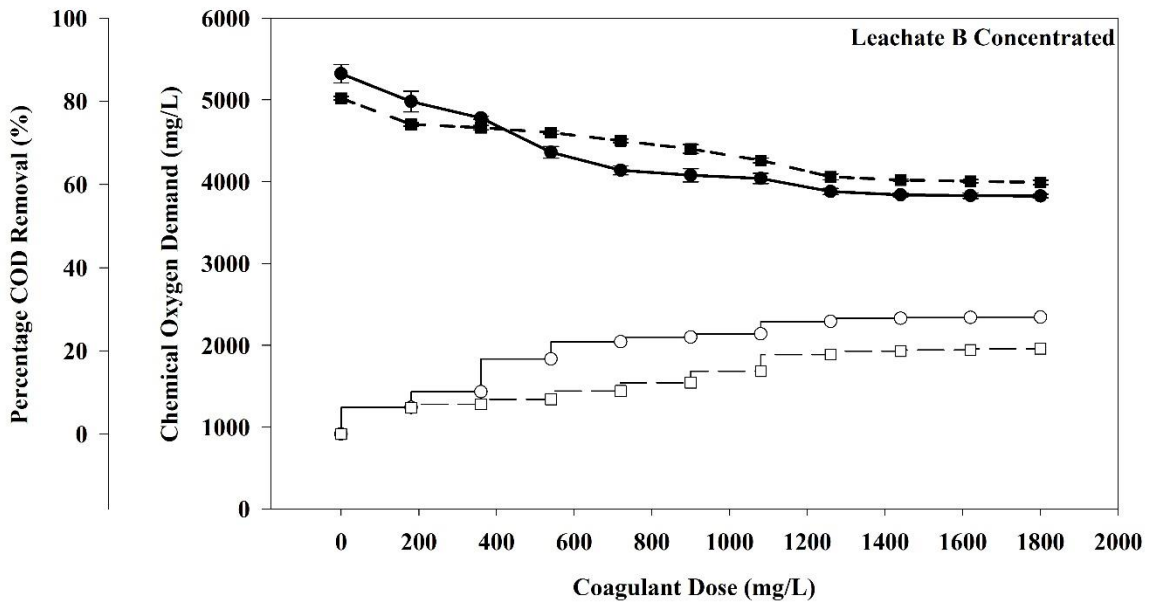
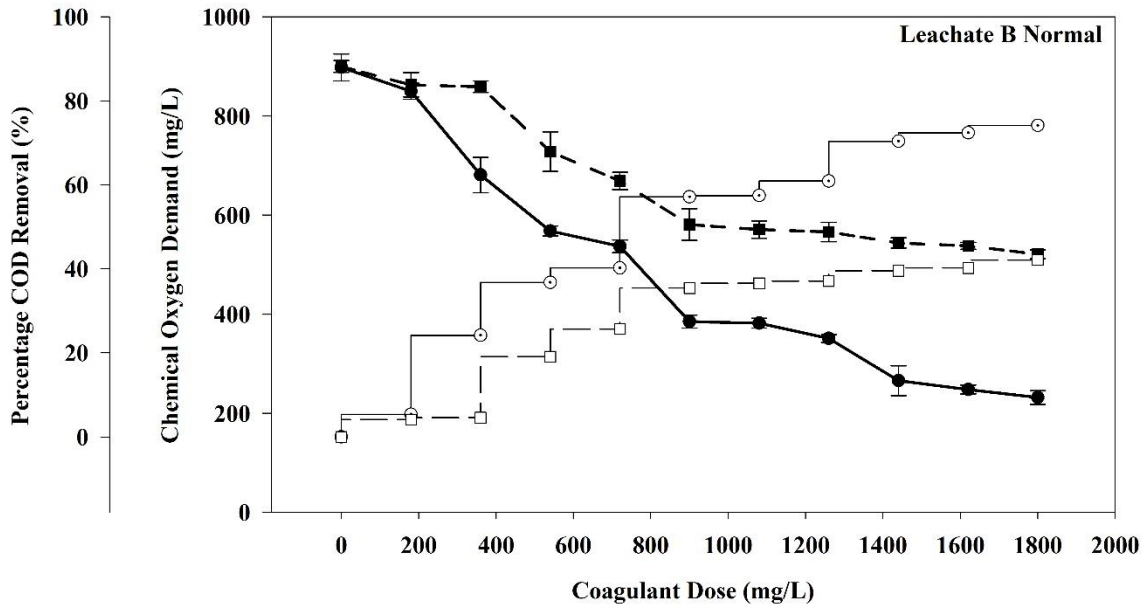
167

168

Figure 1(a): Chemical Oxygen Demand removal from Site A normal and concentrated leachate (error bar represents standard deviation)

169

170 Figures 1(b) is for site B. As shown in Figure 1(b), COD concentration of site B normal leachate
171 decreased from 898 mg/L to 232 mg/L and 521 mg/L by ferric chloride and aluminum sulphate,
172 respectively. And COD concentration of site B concentrated leachate, as shown in figure 1(b),
173 decreased from 5320 mg/L to 3825 mg/L and 5020 mg/L to 3990 mg/L by ferric chloride and
174 aluminum sulphate, respectively. Maximum COD removals of 74.16 % and 28.1% were achieved
175 by ferric chloride for site B normal and concentrated leachates, respectively.



176

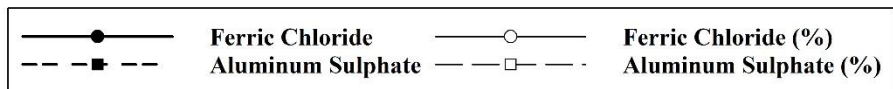
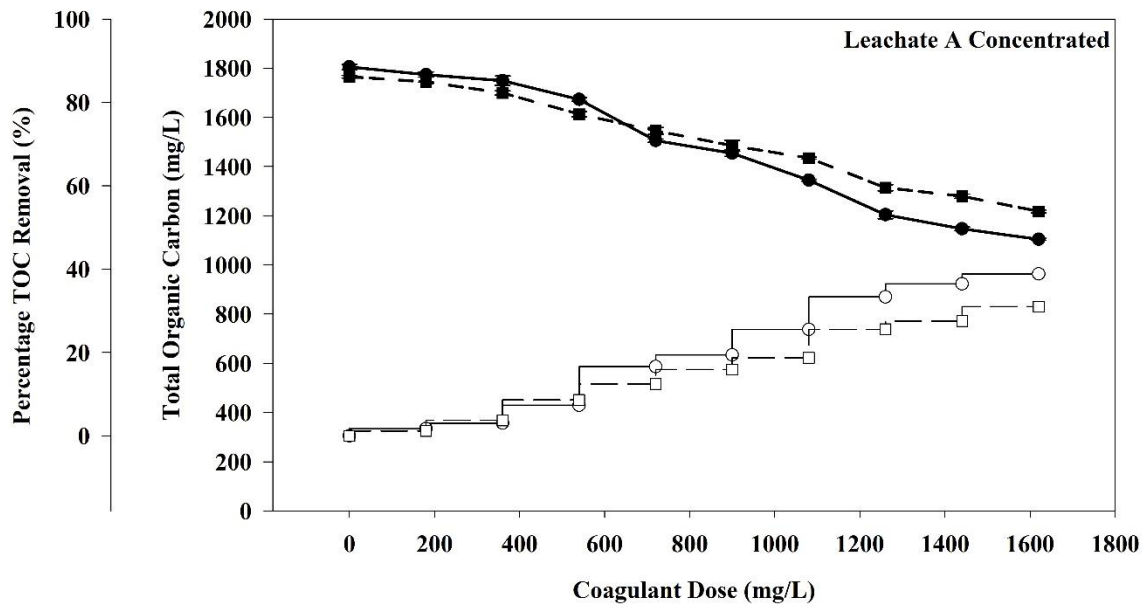
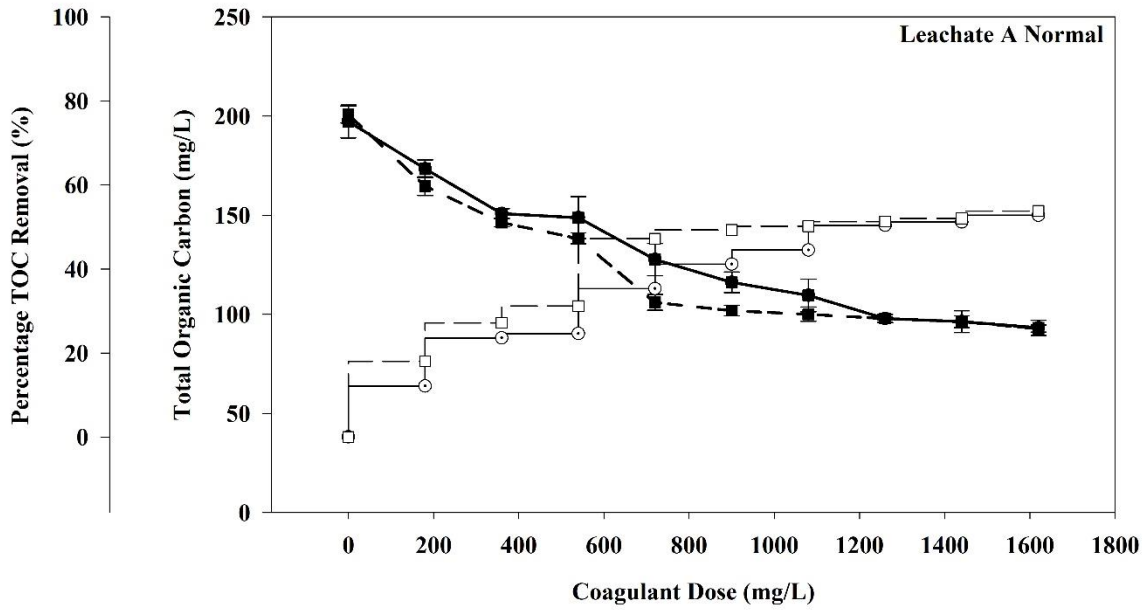
177 *Figure 1(b): Chemical Oxygen Demand Removal from Site B normal and concentrated leachate*

178

179 For a conventional primary sedimentation tank or clarifier, the expected percentage removal for
180 organic matter is 25 – 40% (Tchobanoglous et al., 2003). Although for enhanced treatment such
181 as CEPT, the expected percentage removal is 50 – 70% (Burton et al., 2013). Based on figure 1,
182 treatment performance of both the coagulants for sites A and B normal leachate was in typical
183 range of CEPT method. However, neither aluminum sulphate nor ferric chloride could perform
184 effectively for sites A and B concentrated leachate.

185 Although not a monitored parameter for POTWs discharging limits, TOC is an important
186 parameter to indicate the organic carbon concentration, as organic carbon or the compounds
187 containing organic carbon are the major contributor to UV absorbance.

188 Figure 2 shows TOC removal for normal and concentrated leachate samples from sites A and B
189 by ferric chloride and aluminum sulphate, respectively. Figure 2(a) is for site A. As shown, TOC
190 concentration of normal leachate decreased from about 180 mg/L to 93.2 mg/L and 90.0 mg/L by
191 ferric chloride and aluminum sulphate, respectively. For concentrated leachate, 1800 mg/L of TOC
192 was decreased to 1,103.8 mg/L and 1,217.5 mg/L by ferric chloride and aluminum sulphate,
193 respectively. A maximum of 53.8% and 38.8% of TOC was removed by coagulation from site A
194 normal and concentrated leachates, respectively.



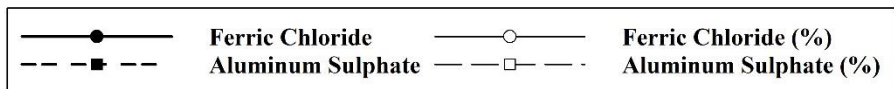
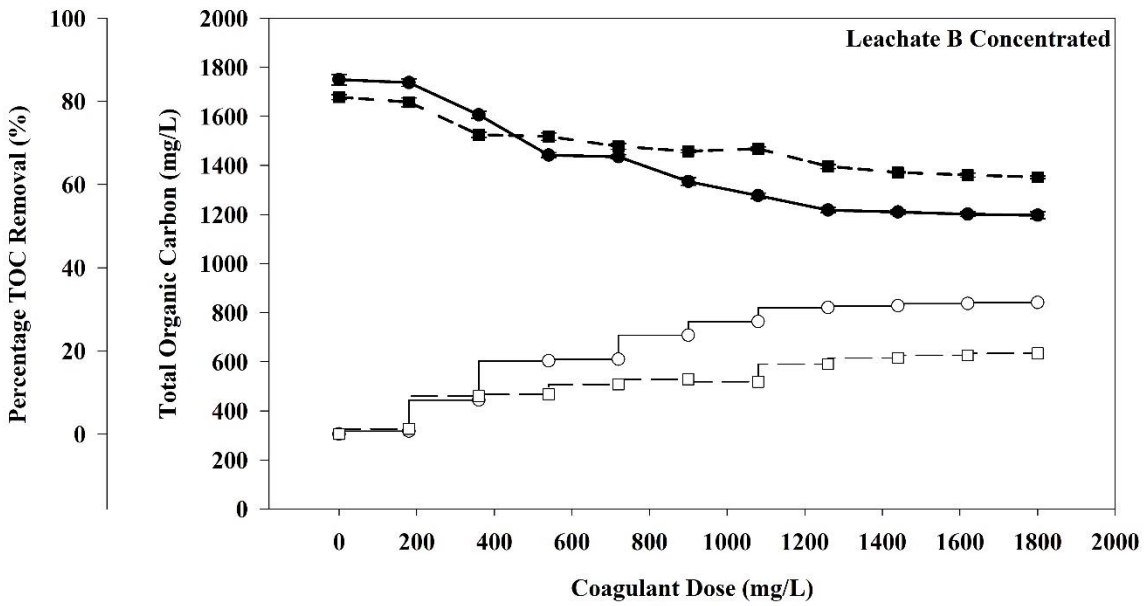
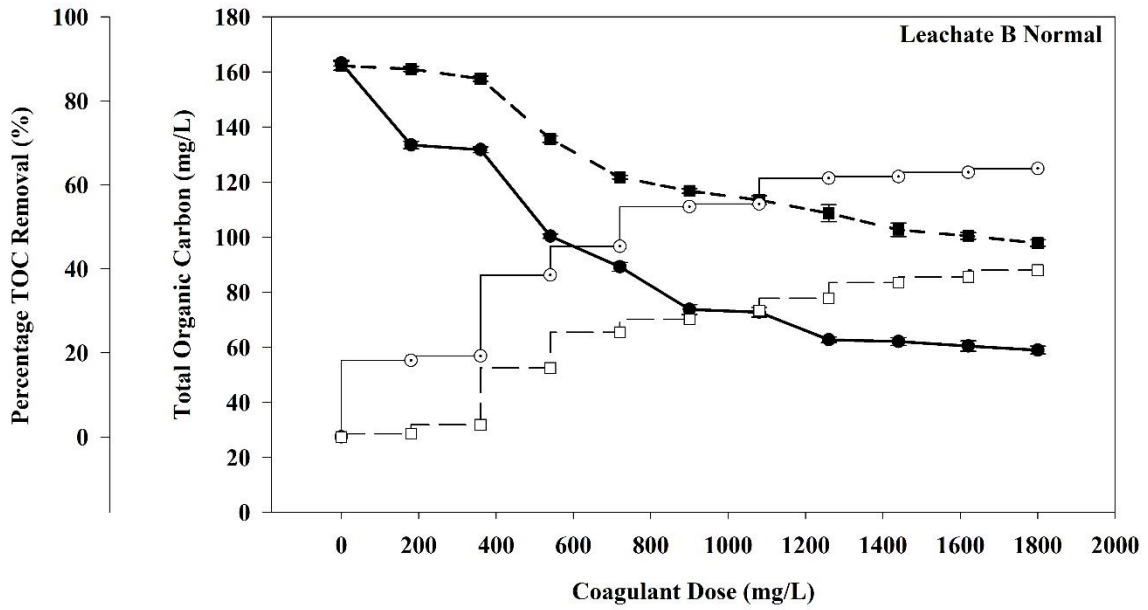
195

196

Figure 2(a): Total Organic Carbon removal from Site A normal and concentrated leachate

197

198 Figures 2(b) is for site B. For normal leachate, the TOC concentration dropped from 133.4 mg/L
199 to 59.0 mg/L and 97.9 mg/L by ferric chloride and aluminum sulphate, respectively. For
200 concentrated leachate, TOC concentration decreased from 1,700.0 mg/L to 1,196.5 mg/L and
201 1,358.0 mg/L by ferric chloride and aluminum sulphate, respectively. A maximum of 63.9% and
202 31.6% of TOC concentration was removed by ferric chloride from site B normal and concentrated
203 leachates, respectively.



204

205

Figure 2(b): Total Organic Carbon removal from Site B normal and concentrated leachate

206

207 Figures 1 and 2 provide the evidence to the effectiveness of CEPT in the removal of organic matter
208 from leachate-sewage co-treatment.

209 Based on several previous published works, it was found that the amount of coagulant dose
210 required for coagulation-flocculation process is directly related to the initial concentration of
211 organic matter in the leachate sample (Assou et al., 2016; Campos et al., 2013; Malathi et al., 2016;
212 Mojiri et al., 2013; Rui and Daud, 2011). Compared to these previous studies, in this study
213 coagulant dose was applied in increment of 200 mg/L until a flat curve was obtained for organic
214 matter removal to evaluate the coagulant dose required for coagulation-flocculation for two
215 leachate samples that have significantly different water quality characteristics (especially organic
216 matter and pH).

217 Previous studies provide following points for leachate treatment with coagulation and flocculation:

218 i) High coagulant dose is required for both ferric and alum for high strength leachate. ii) COD
219 removal is extremely difficult in case of high strength leachate than low strength leachate due to
220 low biodegradability. iii) Ferric chloride tends to perform better in COD removal than aluminum
221 sulphate.

222 Like the studies mentioned above, this study shows that high dosage is required to achieve higher
223 organic matter removal from highly concentrated landfill leachates by CEPT. However, in terms
224 of practical application, using such high coagulant dose may raise concern in term of cost, chemical
225 handling, sludge production and dissolved solids of high coagulant dosage.

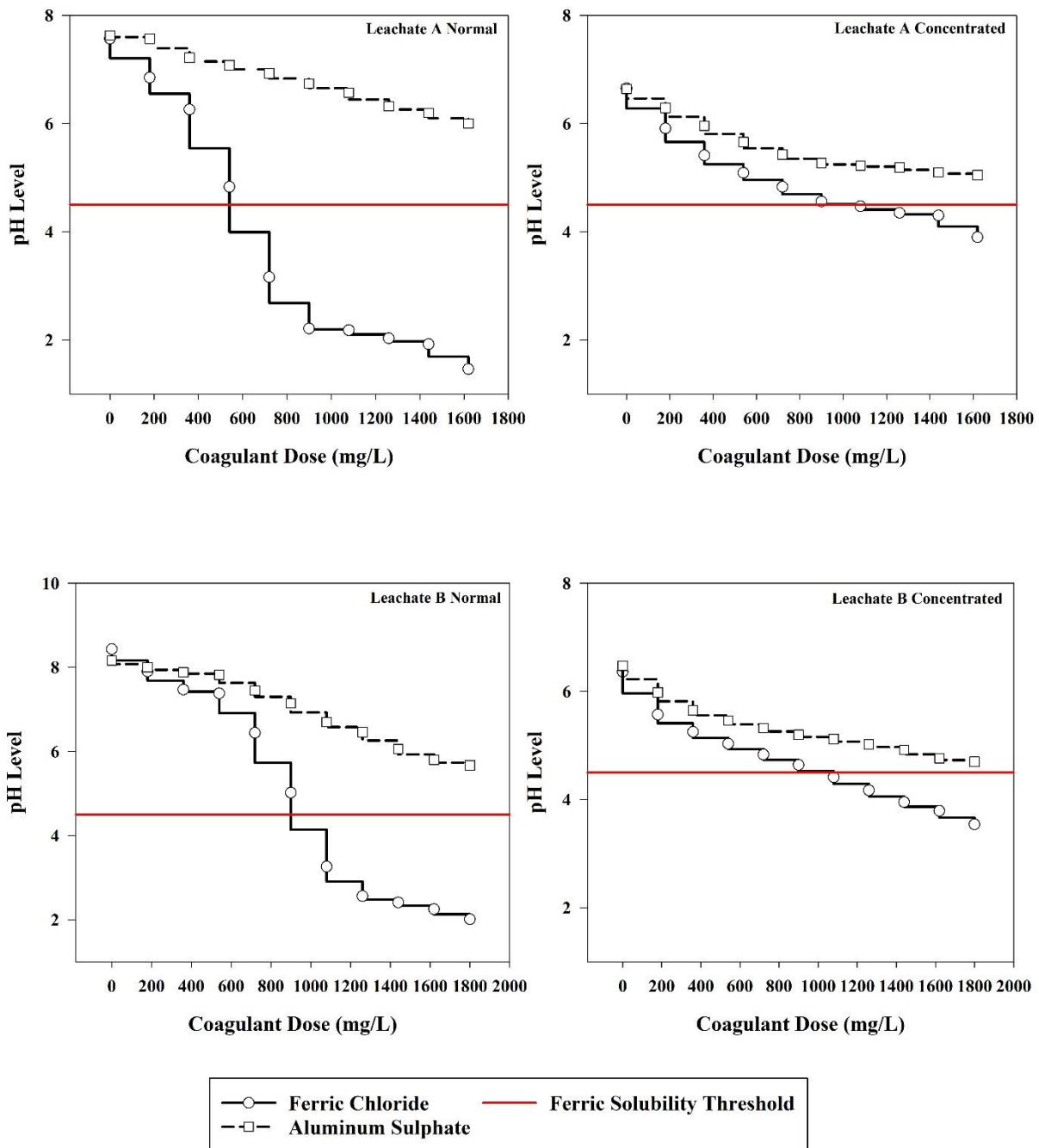
226 In addition, the difference of organics removal rates of normal leachates (up to 74% in terms of
227 COD and 64 % in terms of TOC) and concentrated leachates (up to 32% in terms of COD and

228 39% in terms of TOC) is caused by their different organic compositions. In normal leachate
229 samples (both sites A and B), a considerable portion of COD is contributed by recalcitrant humic
230 substances which are higher molecular weight and prone to be removed with coagulation-
231 flocculation (7). While, concentrated leachate samples (in both sites A and B) contain a
232 significant amount of short chain organic acids (shown in table 1) that tend to stay soluble in a
233 coagulation-flocculation process and limited removal could be achieved (Gawande, 2018). While
234 the percentage removal is lower for the concentrated leachate samples, the mass removal on an
235 unit volume basis is higher than that for normal leachate samples.

236 **3.2 Change in pH**

237 pH is a major factor that affects the effectiveness of the coagulation-flocculation and precipitation
238 processes due to the different solubility of the metal ion at different pH and the availability of
239 hydroxyl group for complexation. For that purpose, the change in pH was recorded to observe
240 the effects of pH on treatment performance and solubility of ferric and aluminum ion in the
241 supernatant after the treatment. Figure 3 shows the change in pH in all four samples by both ferric
242 chloride and aluminum sulphate.

243 As mentioned above, for optimum removal of contaminants, pH for both ferric chloride and
244 aluminum sulphate should be in an optimum range of 5.5 – 8.5 (“Water Treatability Database,”
245 n.d.). If pH is below 5, the solubility of both metal ions will increase and impact the coagulation-
246 flocculation performance.



247

248 *Figure 3: Change in pH due to coagulation for Site A and B, normal and concentrated leachate*

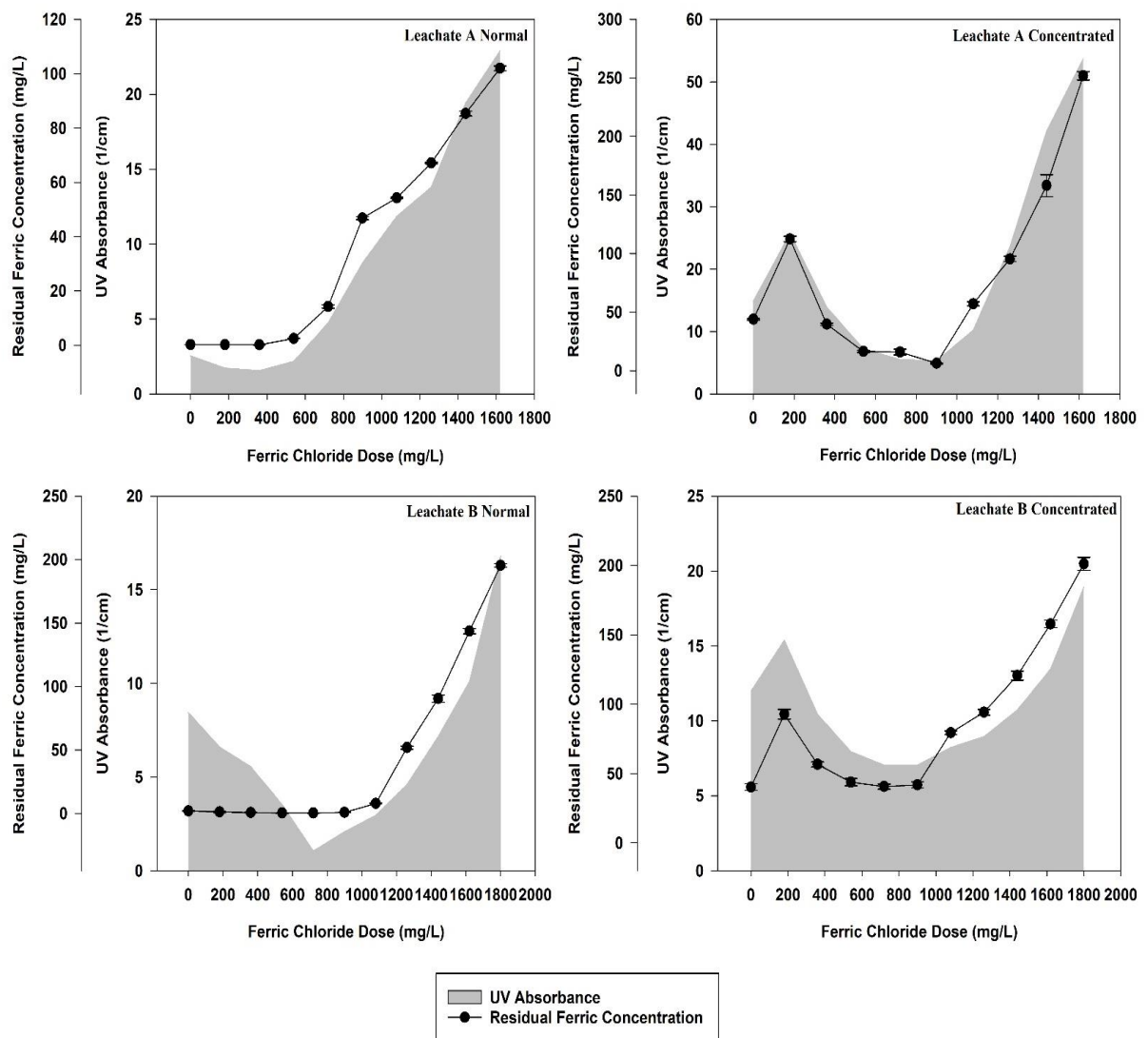
249 As shown in Figure 3, a decrease in pH was observed due to the addition of both ferric chloride
250 and aluminum sulphate. However, different trends were observed for aluminum sulphate and ferric
251 chloride. Aluminum sulphate did not cause any dramatic change in pH for either normal or
252 concentrated leachate from sites A and B. After aluminum sulphate was dosed, the pH decreased
253 from 7.6 to 6 and from 6.6 to 5 for site A normal and concentrated leachate respectively, and for
254 site B, aluminum sulphate lowered the pH from 8.16 to 5.16 and from 6.4 to 4.7 for normal and
255 concentrated leachate, respectively. Different from aluminum-based coagulant, ferric chloride
256 caused much greater pH change, especially for normal leachate samples. The change in pH caused
257 by ferric chloride for normal leachate from sites A and B was found significant. Figure 3 shows
258 that when more than 540 mg/L of ferric chloride was dosed, the pH dropped dramatically to 2 or
259 lower for normal leachate from both sites A and B. Meanwhile, ferric chloride did not have such
260 impact on pH level for concentrated leachate from sites A and B. For concentrated leachate from
261 sites A and B, the pH reduced from 6.6 to 3.9 and from 6.4 to 3.54, respectively. Figure 3 shows
262 that when ferric chloride is dosed in high amounts, it will reduce the pH below 5, which is a
263 solubility threshold for ferric ions, below which hydrolyzed ferric complexes become soluble.

264 The different behaviors of pH change during ferric chloride coagulation between normal and
265 concentrated leachates are believed due to the "buffer effect" of the high level of short chain
266 organic acids in found in leachate samples. Short chain organic acids or Volatile Acids (VAs) are
267 weak organic acids and their conjugate base stay in equilibrium in a solvent (in this case leachate).
268 Volatile acids have lower dissociation constant (pK_a) value which gives them the buffer capacity
269 or resistance (in simple terms) towards the change in pH. Some commonly known volatile acids
270 are acetic acid, butyric acid, propionic acid, etc. These acids are also considered as Volatile Fatty
271 Acids (VFAs) that are typically produced during the acidogenesis phase during decomposition of

272 organic waste in landfills. Volatile acids (VAs) test was conducted for raw leachate sample only
273 to understand how the concentration levels of these acids play a role in change in pH during
274 coagulation by providing a buffer capacity to the leachate. Volatile acids (VAs) test determined
275 that Leachate A and B normal sample had a total VAs concentration of 785 mg/L and 1628 mg/L
276 respectively, while concentrated leachate for A and B had 22,850 mg/L and 27,700 mg/L of VA
277 concentration respectively, as shown in figure S8. Hence, concentrated leachate had significantly
278 higher VAs concentration than normal leachate for both A and B sample. Carbon chain may vary
279 in volatile acids; hence, total volatile acid concentration was measured in mg/L as CH_3COOH
280 (Acetic Acid).

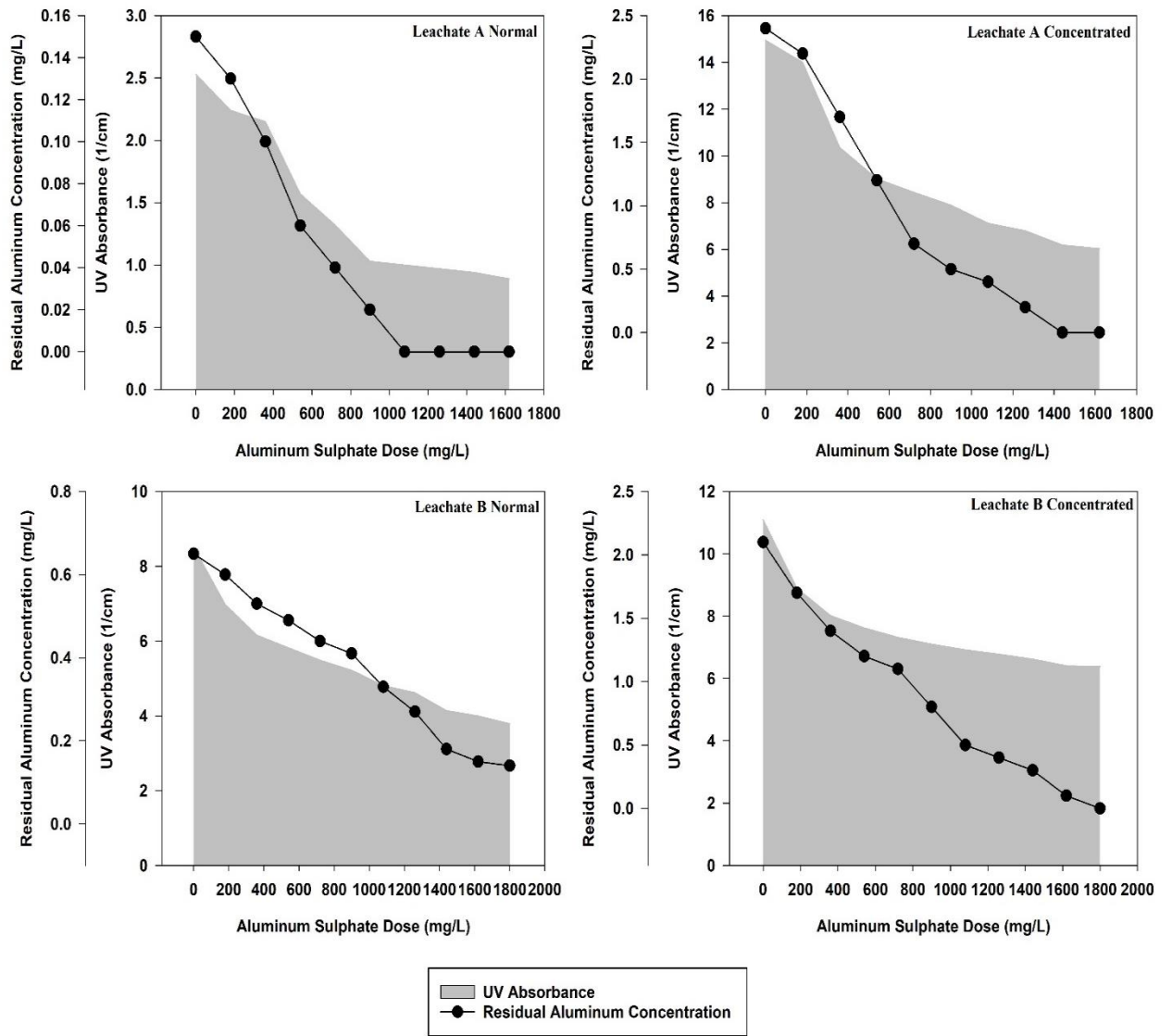
281 By connecting the results from the change in pH and the Volatile Acids test, it can be said that
282 there is a possibility of observing residual soluble metal cations after coagulation, but the
283 observation for normal and concentrated sample would be significantly different. Due to high
284 buffer capacity from Volatile Acids, concentrated leachate samples can handle more ferric than
285 normal before residual Fe increases that results in increase in the UV absorbance post-coagulation.
286 Figures 4 and 5 provide the results obtained for residual ferric and aluminum concentration in the
287 supernatants. It is shown that for all the leachate samples, the concentration of aluminum decreased
288 and reached approximately zero, even for higher coagulant dose. However, a different trend was
289 observed for ferric chloride. For normal leachate from sites A and B, it can be seen from Figure 4
290 that after a certain amount of ferric chloride dose (i.e. 540 mg/L), the residual ferric concentration
291 increased and kept on increasing with the dose. Also, when compared to figure 3, after 540 mg/L
292 of ferric chloride dose, the pH dropped below 5, and as aforementioned, soluble hydrolyzed ferric
293 complexes increases, resulting in increase in residual ferric post-coagulation. While for
294 concentrated leachate from sites A and B, it was found that for the lowest dose, the residual ferric

295 concentration increased. After a higher dose was applied, it decreased, then increased again after
 296 900 mg/L or more dose of ferric chloride was applied. The increase of iron concentration coincides
 297 with the pH drop as shown in figure 3. Similarly, when more than 900 mg/L of ferric chloride was
 298 added for concentrated leachate from site A and B, the pH dropped below 5 (as shown in figure
 299 3), resulting in increased residual ferric post treatment in form of soluble hydrolyzed ferric
 300 complexes.



301
 302 *Figure 4: Change in UV absorbance and residual ferric concentration post-coagulation in Sites*
 303 *A and B, normal and concentrated leachates.*

304
 305
 306
 307
 308



309
 310
 311
 312

Figure 5: Change in UV absorbance and residual aluminum concentration post-coagulation for sites A and B, normal and concentrated leachates.

313 For domestic wastewater, optimum pH for the coagulation process is 6 – 8 for ferric chloride and
314 6 – 9 for aluminum sulphate (Burton et al., 2013) . While for landfill leachate, previous studies
315 show that the optimum pH required is 7 – 10.5 for both ferric chloride and aluminum sulphate
316 (Campos et al., 2013; Farrokhi et al., 2015; Malathi et al., 2016; Rui and Daud, 2011; Wang et al.,
317 2009). In some practices, pH is adjusted before coagulation to improve the removal efficiency of
318 primary treatment. However, POTWs do not always adjust the pH as introduction of extra
319 chemicals may increase the cost of operation, elevate the effluent dissolved solids and may have
320 aftereffects on the downstream processes. Hence, in this study pH adjustment was not carried out.

321 **3.3 Co-precipitation behaviors of ferric chloride as function of pH**

322 Figure 6 illustrates the hypothetical models that can explicate the co-precipitation behaviors of
323 ferric chloride and leachate organic matter in this study under various pH scenarios.

324

325

326

327

328

329

330

331

332

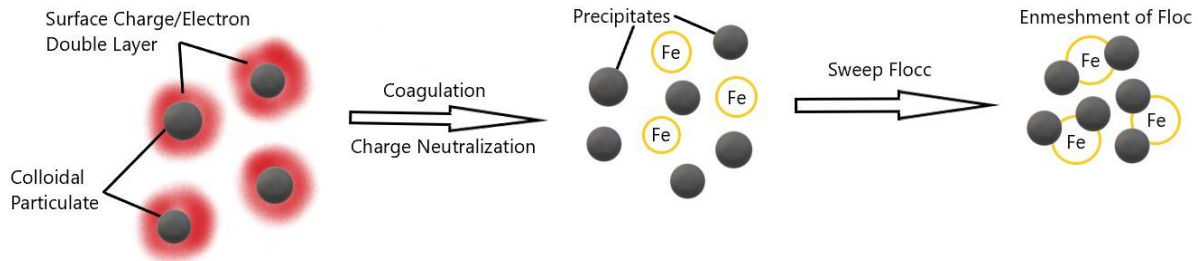
333

334

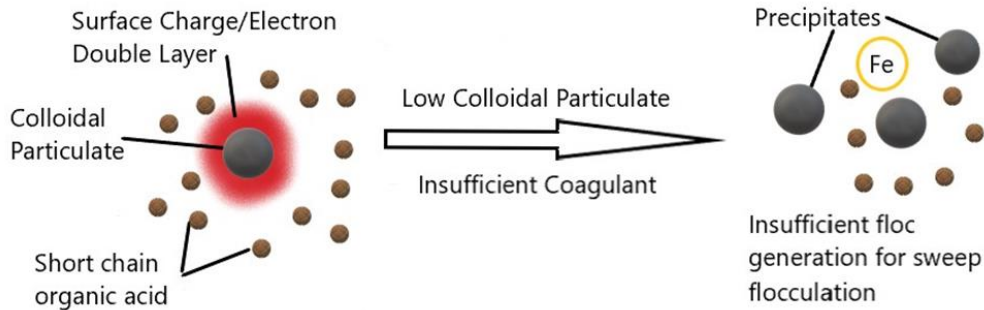
335

336

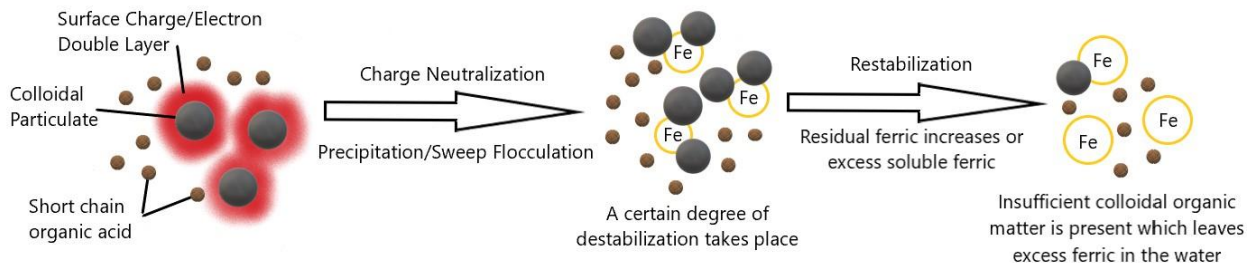
337 (a) scenario 1-a. Complete destabilization and neutralization of anionic organic matter at
 338 optimum coagulant dose
 339



340
 341 (b) scenario 1-b. For leachate A and B concentrated (when 180 mg/L of ferric chloride is added)



342
 343 (c) scenarios 2. Restabilization of hydrolysed species of ferric caused by excess coagulant dose
 344 and acidic pH



345
 346 *Figure 6: Hypothetical models of co-precipitation behaviors under various pH scenarios. (a)*
 347 *scenario 1-a, (b) scenario 1-b, (c) scenario 2.*

348
 349 *Scenario 1: pH is in neutral range (above 6).*

350 Scenario 1 (a). When the pH was in the neutral range (i.e. above 6), the coagulation mechanism
 351 followed precipitation and sweep flocculation for both leachate A and B, normal and concentrated.

352 As shown in figure 3 and figure 4, for leachate A and B normal from coagulant dose 180 mg/L to
353 540 mg/L, precipitation and sweep flocculation was observed and no residual ferric was detected.
354 Similarly, for leachate A and B concentrated from coagulant dose 360 mg/L to 900 mg/L
355 coagulation mechanism followed by precipitation and sweep flocculation, minimal residual ferric
356 concentration was found. Figure 6 (a) shows the stepwise coagulation mechanism for precipitation
357 and sweep flocculation. An effective coagulation occurs when Critical Coagulation Concentration
358 (CCC) is used, where the Critical Coagulation Concentration (CCC) can be defined as the
359 minimum concentration of cations required to neutralize and destabilize the anionic organic matter
360 for coagulation of colloidal particles. Hence, effective coagulation such as this can be achieved
361 when pH of the solution; colloidal concentration in the solution; and Critical Coagulant
362 Concentration (CCC) are in relation with each other as shown in figure S9 taken from (Bratby,
363 2016; Stumm and O'Melia, 1968). for zone 2 and zone 4. Figure 6 (a). Shows the coagulation
364 mechanism for scenario 1 (a), where precipitation and sweep flocculation take place.

365 Scenario 1 (b). However, as shown in Figure 4, for leachate A and B concentrated, when 180 mg/L
366 of ferric chloride was dosed, the residual ferric concentration was found to increase even when the
367 pH was close to 6. Such observation is explained by the concept of Critical Coagulant
368 Concentration (CCC) and colloidal or particulate matter concentration (4). A study (4) discusses
369 the relation between CCC and colloidal concentration and indicated that when the colloidal
370 organic matter concentration is low, the required CCC is higher compared to the case of high
371 colloidal organic matter concentration. Figure S9. shows the relationship between CCC and
372 colloidal concentration (Bratby, 2016; Stumm and O'Melia, 1968).

373 In this study, the organic matter is classified as humic-like substances (high molecular weight
374 compounds) and short chain organic acids. The colloidal organic matter refers to the humic-like

375 substances which are more settleable and can be destabilized much easily than short chain organic
376 acids. Studies have shown that normal leachate and concentrated leachate have different
377 proportions of humic-like substances, and humic-like substance fraction is higher in normal
378 leachate than concentrated leachate (Gawande, 2018; Gupta et al., 2014b; Iskander et al., 2018;
379 Zhao et al., 2013a). In this study, it is shown that organic matter in normal leachate is humic-like
380 substances dominated, while concentrated leachate short chain organic acids dominated. Due to
381 insufficient amount of colloidal concentration and coagulant dosage, this condition is observed for
382 concentrated leachate which has lower proportion of humic-like substance compared to normal
383 leachate. This scenario corresponds to the point X shown in figure S9. The mechanism for this
384 scenario is shown in Figure 6 (b).

385 *Scenario 2: pH is acidic (below 6).*

386 Based on previous theories, optimum pH for ferric chloride coagulation is 5 – 8, where residual
387 metal concentration increased below pH 5 (3,4). Similarly, in this study it was observed that the
388 residual ferric concentration increased when pH dropped below 5. For example, after dosing 540
389 mg/L of ferric chloride, the pH dropped below 5, and the residual metal concentration increased
390 for leachate A and B normal, as shown in figure 3 and figure 4. And after dosing 900 mg/L of
391 ferric chloride, the pH dropped below 5 for leachate A and B concentrated, which resulted in
392 increase in residual ferric concentration, as shown in figure 3 and figure 4. The sudden drop in pH
393 observed by ferric chloride dosing for leachate A and B normal, is due to excess amount of ferric
394 chloride added, which cause the coagulation to go beyond the degree of destabilization, and the
395 flocs get re-stabilized in the water becoming soluble and increasing the residual concentration of
396 ferric chloride (Foster, 1969; Xie and Guan, 2015). After a certain degree of destabilization, the
397 leftover concentration of colloidal organic matter will be insufficient for further coagulation and

398 excess coagulant will stay in the water increasing the turbidity of the supernatant. As shown in
399 figure S9, zone 3 (destabilization region) refers to such condition where the colloidal concentration
400 is too low relative to coagulant dosage. Figure 6 (c) shows the mechanism of how the residual
401 ferric concentration increases due to insufficient leftover colloidal concentration in the water.

402 Due to the varied outcomes in coagulation, theories behind coagulation mechanism can only
403 provide a qualitative approximation of the entire mechanism. Selection of the type and dose of
404 coagulant depends on the characteristics of the coagulant, the concentration and type of
405 particulates, concentration and characteristics of NOM, water temperature, and water quality. Due
406 to the interdependence of these five elements, prediction of the optimum coagulant, combination
407 from characteristics of the particulates and the water quality is not yet possible (“10.2,” 2013; Xie
408 and Guan, 2015).

409 **3.4 UV Absorbance**

410 Figure 4 and 5 represents the result of the UV absorbance at different coagulant doses in normal
411 and concentrated leachates for ferric and aluminum, respectively. As observed the two coagulants
412 showed different patterns for UV absorbance.

413 For aluminum sulphate, the UV absorbance decreases with higher coagulant dose for all cases as
414 shown in Figure 5, along with decrease in residual aluminum concentration.

415 On the contrary, ferric chloride caused significant increase of UV absorbance. In the case of normal
416 leachate from sites A and B, the UV absorbance decreased at lower dosage, but after a certain
417 threshold (when pH drops below 5, resulting in increased soluble hydrolysed ferric complexes),
418 the UV absorbance started to increase proportionally with coagulant dose higher than the threshold
419 point. However, beyond the threshold point, the colour of the supernatant begins to turn yellowish

420 orange and gradually becomes bright red at higher dose of ferric chloride. On the other hand, in
421 the case of concentrated leachate from both sites A and B, a different trend was observed. UV
422 absorbance increased with coagulant dose when 180 mg/L ferric chloride was added, then
423 decreased as more coagulant was dosed. As mentioned in scenario 1(b) in Figure 6, the CCC was
424 lower than the required amount for the colloidal concentration in both concentrated leachate A and
425 B. In turn, the level of destabilization required for floc generation for sweep flocculation was not
426 met, and colloidal fraction stays in a suspended state in the solution without being settled. This
427 colloidal fraction in the supernatant was observed to even pass through 0.45 μm syringe filter.
428 When the supernatants from leachate A and B concentrated were tested for UV absorbance, the
429 suspended colloidal fraction in the solution can cause increase in UV absorbance by means of
430 absorbance or light scattering. However, when the leachate A and B concentrated were subjected
431 to a higher coagulant dose, the required CCC was met and the level of destabilization required for
432 sweep flocculation was achieved and no colloidal fraction was observed in suspended state in the
433 supernatant. Hence, after adding more than 180 mg/L ferric chloride, the UV absorbance was
434 observed to decrease. During experiments, it was observed that the supernatant turns hazy due to
435 formation of micro colloids that do not settle and stay suspended, which can cause the UV
436 absorbance to increase due to light scattering.

437 From Figure 4, the elevation of supernatant UV absorbance coincides with the increase in residual
438 soluble ferric concentration, which indicates a possible relevance between ferric cation and UV
439 absorbance. Similar phenomenon was observed and reported in previous studies that reported the
440 influence of ferric ion in UV absorbance at 254 nm (Doane and Horwáth, 2010; Stefánsson, 2007;
441 Turner and Miles, 2011). Few other studies showed that it was the hydrolysed species of iron (III)
442 and their concentration responsible for UV absorbance (Grieve and Marsden, 2001; Korshin et al.,

443 1997; Monique Meier et al., 1999; Moore, 1988; Weishaar et al., 2003; Wilson, 1959). However,
444 it was found in some studies that the presence of iron (III) along with DOM (NOM in
445 environmental conditions) and the interaction between iron (III) and DOM was the cause of increased
446 UV absorbance (Ghassemi and Christman, 1968; Karathanasis et al., 1988; Maloney et al., 2005;
447 M. Meier et al., 1999; Namjesnik-Dejanovic et al., 2000; Sholkovitz and Copland, 1981; Smal and
448 Misztal, 1996; Tipping, 1981; Vestin et al., 2008). More specifically, the formation of organometal
449 complex compound between ferric and recalcitrant organic matter (or DOM) that hypothetically
450 has characteristic absorption in the UV range. Previous studies have shown metal complexation
451 between organic matter and metal ions and ammonia exist in the natural environment, surface
452 water and wastewater treatment processes, etc. (Buffle et al., 1988; Bundy et al., 2015; Lawrence,
453 2009; Suffet, 1989). Hence, in this study, supported by the previous studies, the phenomenon of
454 metal complexation between ferric and organic matter and its impact on UV absorbance is further
455 explained.

456 In this study, the metal ion refers to ferric (Fe^{+3}) and the ligand is the dissolved organic matter
457 present in the leachate. Ferric cation (Fe^{+3}) has 6 empty orbitals and it can accept 6 electrons from
458 a donor ligand, allowing it to form 6 coordinate covalent bonds with 6 anionic ligands (Lawrence,
459 2009). As the dissolved organic matter have different functional groups that can act as binding sites
460 (electron donors) for metal complexes such as carboxylic ($-\text{COOH}$), phenolic ($-\text{OH}$), amine (NH_2),
461 Nitro ($-\text{NO}$), etc. But the major functional group present is the carboxylic and phenolic group.
462 Certain dissolved organic matter (DOM) model, such as humic acid, also show that metal is
463 partially bonded to water molecule at the oxygen atom as a binding site and partially bound to
464 oxygen present in hydroxyl part of the carboxylic and phenolic group (Buffle et al., 1988). Hence,
465 in this study, the major functional groups, present in the DOM, i.e., carboxylic and phenolic group

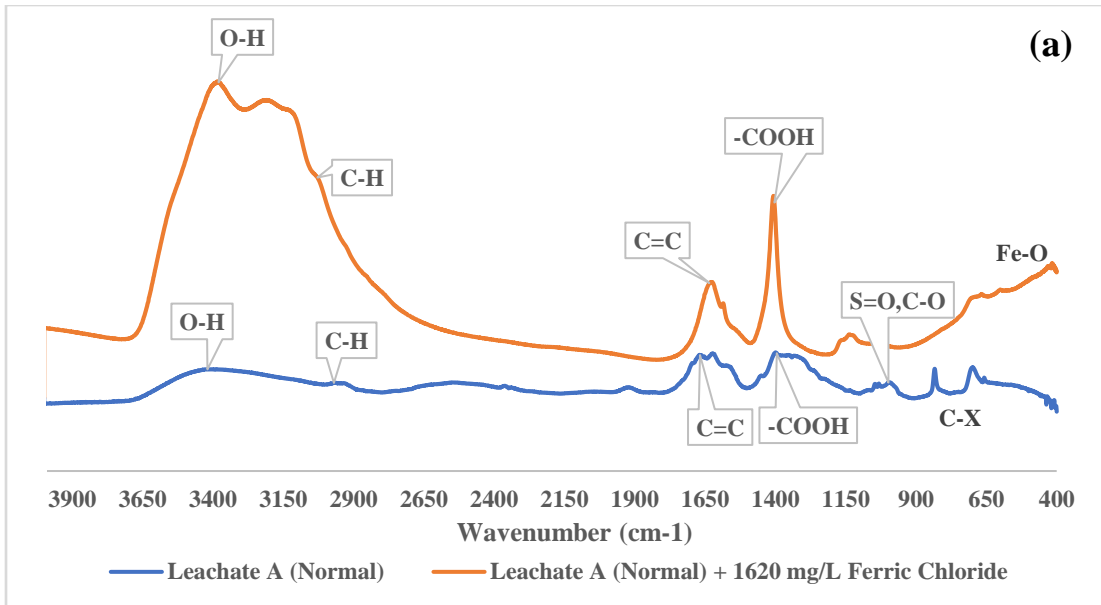
466 have been considered. Elemental analysis of landfill leachate show that oxygen is the second most
467 abundant element in organic compounds (Gawande, 2018). Dissolved Organic Matter (humic
468 substance) consists approximately 30 – 40 % oxygen depending upon the source, which is second
469 to carbon (50 – 60 %) (Iskander et al., 2018). Due to availability and an extra pair of electrons to
470 donate, oxygen presents itself as the most suitable binding site for metal complexes in DOM
471 (humic substance) which is also supported by a recent study (Zhou et al., 2015). Ferric and oxygen
472 from DOM form metal complex with ML_6 (M-Metal and L-Ligand) structure and octahedral
473 geometry (Buffle et al., 1988; Lawrence, 2009). One such example of DOM-iron complexation is
474 Kleinhempel's model of humic substance (Buffle et al., 1988).

475 The ML_6 orbital diagram of the Fe-O coordinate covalent bond is shown in figure S10 (Bauman,
476 1962; Foster, 1969; Graddon, 2017; Lawrence, 2009). When the metal complex is formed, the 3d
477 orbital in ferric splits into e_g^* and t_{2g} orbital with different energy level than before, as explained
478 by crystal field theory and ligand field theory (Gillam and Stern, 1955; Spectroscopy based
479 Adsorption, 2013; Xie and Guan, 2015). The difference in energy is represented by Δ in the figure.
480 Compared to the initial ferric orbital, the energy required by an electron to jump from t_{2g} to e_g
481 increases when the 3d orbital splits into e_g^* and t_{2g} (Ashcroft and Mortimer, 1970; Bamford, 2014;
482 Basolo and Johnson, 1986; Foster, 1969; Kettle, 1969; Kramer and Duinker, 1984). Due to this
483 increase, electron absorb higher amount of energy in form of photons from light to jump from t_{2g}
484 to e_g^* . In this study, it is hypothesized that the energy required to make the electron transition,
485 matches that of UV light in electromagnetic spectrum. Hence, it suggests that when metal
486 complexes are formed with Fe-O bond, the UV absorbance increases.

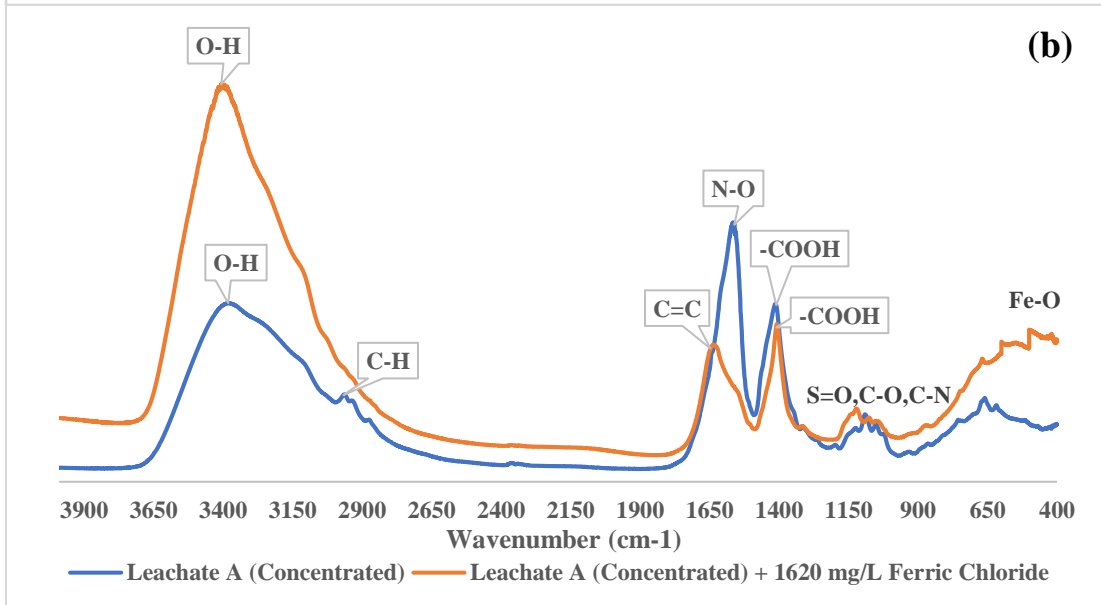
487 **3.5 FT-IR Analysis**

488 FT-IR spectroscopy serves as a tool to identify the organic functional groups present in the sample.
489 Figures 7 (a), (b), (c) and (d) show the FTIR spectra for normal and concentrated leachates from
490 sites A and B, before and after ferric chloride coagulation. It is shown that functional groups such
491 as alcohol and carboxylic (-OH), alkane (C-H), alkene (C=C), sulfoxide (S=O), and halogen
492 compound (C-X) were found in normal leachate from sites A and B. In addition to similar
493 functional groups with normal leachates, ester (C-O) and nitro compound (N-O) were found in
494 concentrated leachates for sites A and B (“IR Spectrum Table & Chart,” n.d.).

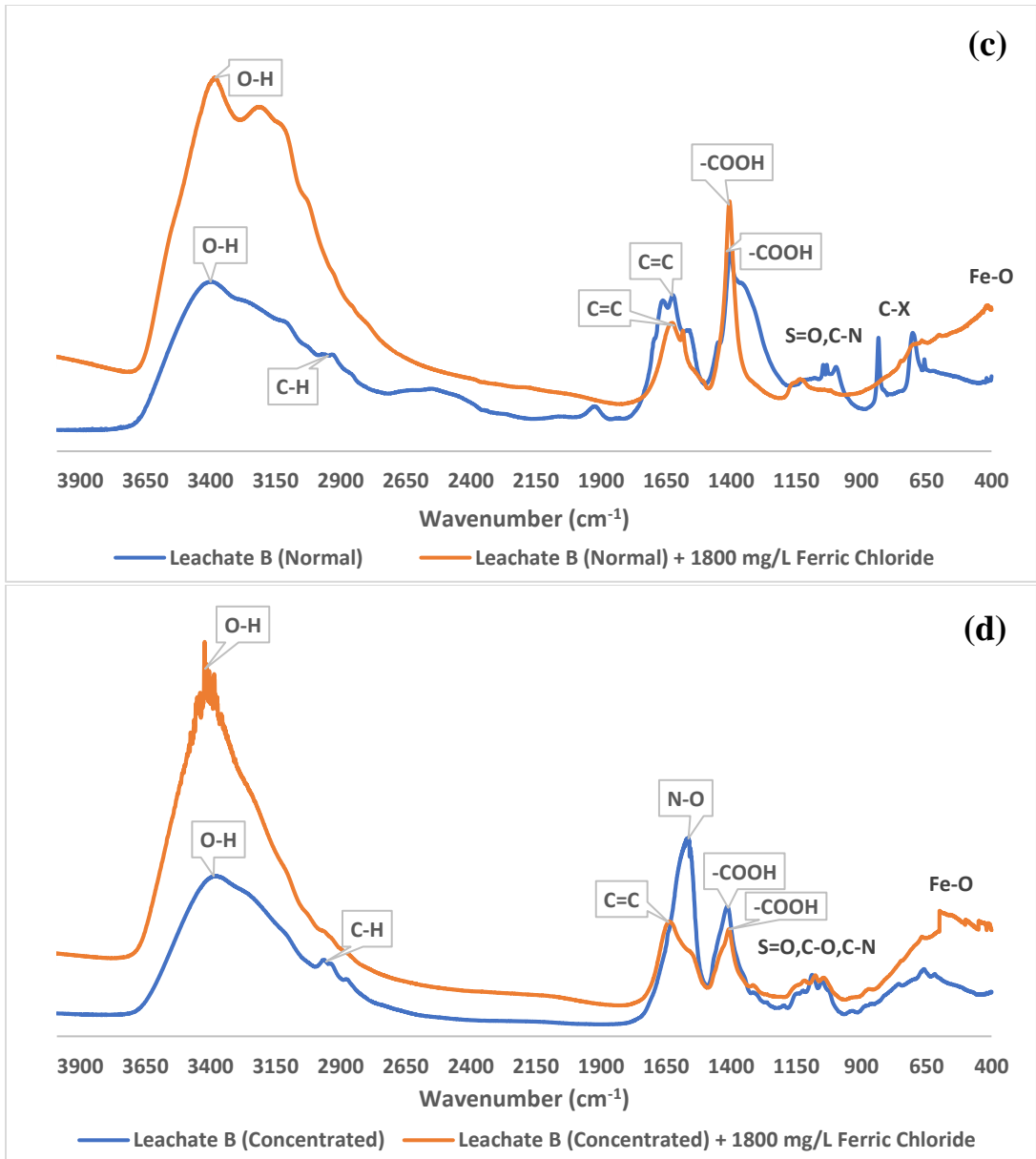
495 Various studies on different materials have shown that Fe-O bond mostly exists in the region 600
496 - 400 cm^{-1} or below 400 cm^{-1} IR spectrum region and also the structure of the Fe-DOM (Fe-Humic)
497 complex (Hossain et al., 2017; Kim and Park, 2002; Novoselova, 2016; Ou et al., 2009; Rahman
498 et al., 2010; Stevenson and Fitch, 1986; Zhou et al., 2015). These studies have used different ferric
499 solution and organic compounds to analyse the Fe-O bond. Similarly, in this study it was observed
500 that the absorbance peak increased post-treatment in the region below 600 cm^{-1} for the leachate
501 sample treated with ferric chloride. This increase in absorbance below 600 cm^{-1} wave number is
502 hypothesized to be due to Fe-O bond stretch that occurs in the metal complex formed from covalent
503 co-ordinate between ferric ion and oxygen in organic ligands (in this case humic
504 acid/macromolecules). Not only the peak increased with increase in ferric dosage, but also it was
505 noticed that the peak for O-H also increased and shifted towards lower wave number, indicating
506 that the ferric cation maybe causing an increase in the stretch of O-H bond. It was also observed
507 that for the raw sample, the peak in the region 600 - 400 cm^{-1} shows a decreasing trend for both
508 normal and concentrated leachate from sites A and B. While the coagulation-flocculation
509 supernatant from highest coagulant dose shows a clear peak in that region. The above evidence
510 indicates and supports the theory of possible metal complexation between ferric cation and DOM.



511



512
513
514
515
516
517
518
519
520
521
522
523
524
525



526

527

528

529

530

531

532

533

Figure 7: FT – IR spectra. (a) normal leachate from site A, (b) concentrated leachate from site A, (c) normal leachate from site B, (d) concentrated leachate from site B.

534 **4. CONCLUSIONS**

535 In this study, lab scale tests with coagulants were conducted for blended landfill leachate and
536 sewage to mimic the co-treatment in POTWs. Main findings are as below:

537 1) Ferric coagulant can cause significant UV abs. increase while aluminium cannot. The high UV
538 abs. coincide with high residual ferric concentration. It is hypothetically believed that the UV
539 abs. increase is caused by the complexation of soluble ferric and leachate organic matter, which
540 produce the Fe-O complex with the molecular structure that has characteristic absorption in
541 the UV range. The Fe-O structure is proved by FT-IR spectra.

542 2) Both aluminium and ferric coagulants perform well for organic matter removal in landfill
543 leachate. For both aluminium and ferric coagulants, organic matter removal efficacy for
544 normal leachate is better than concentrated leachate. For normal leachate, 64% TOC and 74%
545 of COD removal were achieved. For concentrated leachate, 39% TOC and 32% of COD
546 removal were achieved. However, in terms of mass-based removal per unit volume of sample,
547 concentrated leachate had higher organic matter removal than normal leachate samples.

548 3) Both aluminium and ferric coagulants lower the pH during the coagulation-flocculation
549 process for landfill leachate. Ferric reduce pH more than aluminium in all cases. Particularly,
550 pH value was dropped dramatically to less than 2 by ferric for normal leachate. No dramatic
551 pH drop was observed for the concentrated leachates due to the buffer effects of high levels of
552 organic acids (weak acids).

553 4) The relationship between colloidal destabilization and coagulant dose under various pH
554 scenarios can be elucidated by theoretical models presented in this study, such as the critical
555 coagulant concentration required to completely destabilize the anionic organic molecules
556 while not exceeding the maximum allowable coagulant dose beyond which concentration of

557 residual metal cations can increase and interact with organic macromolecules to exacerbate
558 UV absorbance.

559 **Appendix A.** Supporting Information.

560 **ACKNOWLEDGEMENTS**

561 The authors gratefully acknowledge Mr. Roger Green at Waste Management Inc. for providing
562 landfill leachate samples, Ms. Jess Liao at City of Beaumont for providing sewage samples, and
563 Drs. Xiangyang Lei and Clayton Jeffryes at Lamar University for sharing research facilities.

564 The authors acknowledge research funding from National Science Foundation (#1760710) and
565 Waste Management Inc.

566

567 **REFERENCES**

- 568 Aarts, T., 1994. Alternative Approaches for Leachate Treatment [WWW Document]. Waste360.
569 URL http://www.waste360.com/mag/waste_alternative_approaches_leachate (accessed
570 2.15.20).
- 571 Aiyuk, S., Amoako, J., Raskin, L., van Haandel, A., Verstraete, W., 2004. Removal of carbon
572 and nutrients from domestic wastewater using a low investment, integrated treatment
573 concept. *Water Res.* 38, 3031–3042. <https://doi.org/10.1016/j.watres.2004.04.040>
- 574 Ashcroft, S.J., Mortimer, C.T., 1970. Thermochemistry of transition metal complexes. Academic
575 Press, London.
- 576 Assou, M., Fels, L.E., Asli, A.E., Fakidi, H., Souabi, S., Hafidi, M., 2016. Landfill leachate
577 treatment by a coagulation–flocculation process: effect of the introduction order of the
578 reagents. *Desalination Water Treat.* 57, 21817–21826.
579 <https://doi.org/10.1080/19443994.2015.1127779>
- 580 Bamford, C.H., 2014. Reactions of Metallic Salts and Complexes, and Organometallic
581 Compounds. Elsevier, Amsterdam.
- 582 Basolo, F., Johnson, R.C., 1986. Coordination chemistry. Science Reviews, Washington.
- 583 Basu, S., Page, J., Wei, I., 2007. UV disinfection of treated wastewater effluent: influence of
584 color, reactivation and regrowth of coliform bacteria.
- 585 Bauman, R.P., 1962. Absorption spectroscopy. Wiley, New York.
- 586 Bolyard, S., 2017. State of Practice of Landfill Leachate Management and Treatment in the U.S.
587 *Environ. Res. Educ. Found.* URL [https://erefdn.org/state-practice-landfill-leachate-](https://erefdn.org/state-practice-landfill-leachate-management-treatment-u-s/)
588 [management-treatment-u-s/](https://erefdn.org/state-practice-landfill-leachate-management-treatment-u-s/) (accessed 9.15.17).

589 Bratby, J., 2016. Coagulation and Flocculation in Water and Wastewater Treatment. IWA
590 Publishing.

591 Bridgewater, L., Association, A.P.H., Association, A.W.W., Federation, W.E., 2012. Standard
592 Methods for the Examination of Water and Wastewater. American Public Health
593 Association.

594 Buffle, J., Chalmers, R.A., Masson, M.R., Midgley, D., 1988. Complexation reactions in aquatic
595 systems: an analytical approach. E. Horwood, Chichester.

596 Bundy, R.M., Abdulla, H.A.N., Hatcher, P.G., Biller, D.V., Buck, K.N., Barbeau, K.A., 2015.
597 Iron-binding ligands and humic substances in the San Francisco Bay estuary and
598 estuarine-influenced shelf regions of coastal California. *Mar. Chem.*, SCOR WG 139:
599 Organic Ligands – A Key Control on Trace Metal Biogeochemistry in the Ocean 173,
600 183–194. <https://doi.org/10.1016/j.marchem.2014.11.005>

601 Burton, F.L., Tchobanoglous, G., Tsuchihashi, R., Stensel, H.D., Inc, M.& E., 2013. Wastewater
602 Engineering: Treatment and Resource Recovery. McGraw-Hill Education, New York.

603 Campos, J.C., Machado, B. da S., Blonski, M.E.D., Bila, D.M., Ferreira, J.A., 2013. Evaluation
604 of coagulation/flocculation process in the landfill leachate treatment at the Municipal
605 Wastewater Treatment Plant. *Ambiente E Agua - Interdiscip. J. Appl. Sci.* 8, 43–53.

606 Chagnon, F.J.F., Harleman, D.R.F., 2005. Chemically Enhanced Primary Treatment of
607 Wastewater, in: *Water Encyclopedia*. John Wiley & Sons, Inc., Hoboken.
608 <https://doi.org/10.1002/047147844X.ww63>

609 De Feo, G., De Gisi, S., Galasso, M., 2008. Definition of a practical multi-criteria procedure for
610 selecting the best coagulant in a chemically assisted primary sedimentation process for
611 the treatment of urban wastewater. *Desalination* 230, 229–238.
612 <https://doi.org/10.1016/j.desal.2007.12.003>

613 Doane, T.A., Horwath, W.R., 2010. Eliminating interference from iron(III) for ultraviolet
614 absorbance measurements of dissolved organic matter. *Chemosphere* 78, 1409–1415.
615 <https://doi.org/10.1016/j.chemosphere.2009.12.062>

616 Farrokhi, M., Dindarloo, K., Jamali, H.A., 2015. Optimization of coagulation-flocculation
617 process for mature landfill leachate treatment using response surface methodology
618 (RSM). *Res. J. Pharm. Biol. Chem. Sci.* 6, 128.

619 Foster, R., 1969. Organic charge-transfer complexes. Academic Press, London.

620 Gawande, S., 2018. Characterization of Leachates from Elevated Temperature Landfills (ETLFs)
621 and Dissolved Organic Matter (DOM) - ProQuest.

622 Ghassemi, M., Christman, R.F., 1968. Properties of the Yellow Organic Acids of Natural
623 Waters1. *Limnol. Oceanogr.* 13, 583–597. <https://doi.org/10.4319/lo.1968.13.4.0583>

624 Gillam, A.E., Stern, E.S., 1955. An Introduction to Electronic Absorption Spectroscopy in
625 Organic Chemistry. Arnold, London.

626 Graddon, D.P., 2017. An Introduction to Co-Ordination Chemistry: International Series of
627 Monographs in Inorganic Chemistry. Elsevier, Burlington.

628 Grieve, I.C., Marsden, R.L., 2001. Effects of forest cover and topographic factors on TOC and
629 associated metals at various scales in western Scotland. *Sci. Total Environ.* 265, 143–
630 151. [https://doi.org/10.1016/S0048-9697\(00\)00655-0](https://doi.org/10.1016/S0048-9697(00)00655-0)

631 Gupta, A., Zhao, R., Novak, J.T., Douglas Goldsmith, C., 2014a. Application of Fenton's reagent
632 as a polishing step for removal of UV quenching organic constituents in biologically
633 treated landfill leachates. *Chemosphere* 105, 82–86.
634 <https://doi.org/10.1016/j.chemosphere.2013.12.066>

635 Gupta, A., Zhao, R., Novak, J.T., Goldsmith, C.D., 2014b. Variation in organic matter
636 characteristics of landfill leachates in different stabilisation stages. *Waste Manag. Res.*
637 32, 1192–1199. <https://doi.org/10.1177/0734242X14550739>

638 Harleman, D.R.F., Murcott, S., 1999. The role of physical-chemical wastewater treatment in the
639 mega-cities of the developing world. *Water Sci. Technol.* 40, 75–80.
640 [https://doi.org/10.1016/S0273-1223\(99\)00487-4](https://doi.org/10.1016/S0273-1223(99)00487-4)

641 Hossain, M.S., Zakaria, C.M., Zahan, M.K., 2017. Synthesis and Characterization with
642 Antimicrobial Activity Studies on some Transition Metal Complexes of N, O Donor
643 Novel Schiff Base Ligand. *J. Sci. Res.* 9, 209–218. <https://doi.org/10.3329/jsr.v9i2.29780>

644 IR Spectrum Table & Chart [WWW Document], n.d. . Sigma-Aldrich. URL
645 [https://www.sigmaaldrich.com/technical-documents/articles/biology/ir-spectrum-](https://www.sigmaaldrich.com/technical-documents/articles/biology/ir-spectrum-table.html)
646 [table.html](https://www.sigmaaldrich.com/technical-documents/articles/biology/ir-spectrum-table.html) (accessed 12.28.18).

647 Iskander, S.M., Zhao, R., Pathak, A., Gupta, A., Pruden, A., Novak, J.T., He, Z., 2018. A review
648 of landfill leachate induced ultraviolet quenching substances: Sources, characteristics,
649 and treatment. *Water Res.* 145, 297–311. <https://doi.org/10.1016/j.watres.2018.08.035>

650 Jiang, J.-Q., 2015. The role of coagulation in water treatment. *Curr. Opin. Chem. Eng.* 8, 36(9).

651 Jordão, E.P., Volschan, I., 2004. Cost-effective solutions for sewage treatment in developing
652 countries--the case of Brazil. *Water Sci. Technol. J. Int. Assoc. Water Pollut. Res.* 50,
653 237–242.

654 Karathanasis, A.D., Evangelou, V.P., Thompson, Y.L., 1988. Aluminum and Iron Equilibria in
655 Soil Solutions and Surface Waters of Acid Mine Watersheds. *J. Environ. Qual.* 17, 534–
656 543. <https://doi.org/10.2134/jeq1988.00472425001700040003x>

657 Karidis, A., 2016. Landfill Leachate Management Impacted by Changes at Wastewater
658 Treatment Plants [WWW Document]. Waste360. URL
659 [http://www.waste360.com/leachate/landfill-leachate-management-impacted-changes-](http://www.waste360.com/leachate/landfill-leachate-management-impacted-changes-wastewater-treatment-plants)
660 [wastewater-treatment-plants](http://www.waste360.com/leachate/landfill-leachate-management-impacted-changes-wastewater-treatment-plants) (accessed 12.1.17).

661 Kettle, S.F.A., 1969. *Coordination Compounds*. Appleton-Century-Crofts.

662 Kim, Y.J., Park, C.R., 2002. Analysis of Problematic Complexing Behavior of Ferric Chloride
663 with *N, N*-Dimethylformamide Using Combined Techniques of FT-IR, XPS, and
664 TGA/DTG. *Inorg. Chem.* 41, 6211–6216. <https://doi.org/10.1021/ic011306p>

665 Korshin, G.V., Li, C.-W., Benjamin, M.M., 1997. Monitoring the properties of natural organic
666 matter through UV spectroscopy: A consistent theory. *Water Res.* 31, 1787–1795.
667 [https://doi.org/10.1016/S0043-1354\(97\)00006-7](https://doi.org/10.1016/S0043-1354(97)00006-7)

668 Kramer, C.J.M., Duinker, J.C. (Eds.), 1984. *Complexation of trace metals in natural waters*.
669 Springer Netherlands, Dordrecht. <https://doi.org/10.1007/978-94-009-6167-8>

670 Lawrence, G.A., 2009. *Introduction to Coordinate Chemistry*. John Wiley & Sons, Ltd, New
671 York.

672 Malathi, R., Shoba, B., Sindhuja, P., V, V., 2016. Landfill Leachate Treatment by Coagulation
673 and Flocculation Process. *Cafet Innova* 9, 885–887.

674 Maloney, K.O., Morris, D.P., Moses, C.O., Osburn, C.L., 2005. The Role of Iron and Dissolved
675 Organic Carbon in the Absorption of Ultraviolet Radiation in Humic Lake Water.
676 *Biogeochemistry* 75, 393–407. <https://doi.org/10.1007/s10533-005-1675-3>

677 Meier, Monique, Namjesnik-Dejanovic, K., Maurice, P.A., Chin, Y.-P., Aiken, G.R., 1999.
678 Fractionation of aquatic natural organic matter upon sorption to goethite and kaolinite.
679 *Chem. Geol.* 157, 275–284. [https://doi.org/10.1016/S0009-2541\(99\)00006-6](https://doi.org/10.1016/S0009-2541(99)00006-6)

680 Meier, M., Namjesnik-Dejanovic, K., Maurice, P.A., Chin, Y.-P., Aiken, G.R., 1999.
681 Fractionation of aquatic natural organic matter upon sorption to goethite and kaolinite.
682 Chem. Geol. 157, 275–284. [https://doi.org/10.1016/S0009-2541\(99\)00006-6](https://doi.org/10.1016/S0009-2541(99)00006-6)
683 Mojiri, A., Aziz, H.A., Shuokr, Q.A., 2013. Trends in Physical-Chemical Methods for Landfill
684 Leachate Treatment. Int. J. Sci. Res. Environ. Sci. 1, 16–25.
685 <http://dx.doi.org/10.12983/ijres-2013-p016-025>
686 Moore, T.R., 1988. DISSOLVED IRON AND ORGANIC MATTER IN NORTHERN
687 PEATLANDS. Soil Sci. 145, 70–76.
688 Namjesnik-Dejanovic, K., Maurice, P.A., Aiken, G.R., Cabaniss, S., Chin, Y.-P., Pullin, M.J.,
689 2000. Adsorption and fractionation of a muck fulvic acid on kaolinite and goethite at pH
690 3, 7, 6, and 8. Soil Sci. 165, 545–559. <https://doi.org/10.1097/00010694-200007000-00003>
691 Novoselova, L.Yu., 2016. Hematite nanopowder obtained from waste: Iron-removal sludge.
692 Powder Technol. 287, 364–372. <https://doi.org/10.1016/j.powtec.2015.10.020>
693 Ou, X., Chen, S., Quan, X., Zhao, H., 2009. Photochemical activity and characterization of the
694 complex of humic acids with iron(III). J. Geochem. Explor. 102, 49–55.
695 <https://doi.org/10.1016/j.gexplo.2009.02.003>
696 spectroscopy Based on Absorption [WWW Document], 2013. . Chem. Libr. URL
697 [https://chem.libretexts.org/Textbook_Maps/Analytical_Chemistry_Textbook_Maps/Map](https://chem.libretexts.org/Textbook_Maps/Analytical_Chemistry_Textbook_Maps/Map%3A_Analytical_Chemistry_2.0_(Harvey)/10_Spectroscopic_Methods/10.2%3A_Spectroscopy_Based_on_Absorption)
698 [%3A_Analytical_Chemistry_2.0_\(Harvey\)/10_Spectroscopic_Methods/10.2%3A_Spectroscopy_Based_on_Absorption](https://chem.libretexts.org/Textbook_Maps/Analytical_Chemistry_Textbook_Maps/Map%3A_Analytical_Chemistry_2.0_(Harvey)/10_Spectroscopic_Methods/10.2%3A_Spectroscopy_Based_on_Absorption) (accessed 11.13.17).
699
700 Rahman, M.A., Alam, A.S., Abu, H., Md., Rahim, A., 2010. Characterization of humic acid from
701 the river bottom sediments of Burigonga: Complexation studies of metals with humic
702 acid. Pak. J. Anal. Environ. Chem. 11, 42–52.
703 Rui, L.M., Daud, Z.B., 2011. Efficiency of the Coagulation-Flocculation for the Leachate
704 Treatment. OIDA Int. J. Sustain. Dev. 2, 85–90.
705 Sholkovitz, E.R., Copland, D., 1981. The coagulation, solubility and adsorption properties of Fe,
706 Mn, Cu, Ni, Cd, Co and humic acids in a river water. Geochim. Cosmochim. Acta 45,
707 181–189. [https://doi.org/10.1016/0016-7037\(81\)90161-7](https://doi.org/10.1016/0016-7037(81)90161-7)
708 Smal, H., Misztal, M., 1996. Soil solution chemistry in the profiles of forest and arable light
709 textured soils, S.E. Poland. Appl. Geochem., Environmental Geochemistry 11, 81–85.
710 [https://doi.org/10.1016/0883-2927\(95\)00095-X](https://doi.org/10.1016/0883-2927(95)00095-X)
711 Stefánsson, A., 2007. Iron(III) Hydrolysis and Solubility at 25 °C. Environ. Sci. Technol. 41,
712 6117–6123. <https://doi.org/10.1021/es070174h>
713 Stevenson, F.J., Fitch, A., 1986. Chemistry of Complexation of Metal Ions with Soil Solution
714 Organics I. Interact. Soil Miner. Nat. Org. Microbes sssaspecialpubl, 29–58.
715 <https://doi.org/10.2136/sssaspepub17.c2>
716 Stumm, W., O'Melia, C.R., 1968. Stoichiometry of Coagulation. J. Am. Water Works Assoc. 60,
717 514–539.
718 Suffet, I., 1989. Aquatic Humic Substances: Influence on Fate and Treatment of Pollution.
719 American Chemical Society, Washington.
720 Tchobanoglous, G., Burton, F.L., Stensel, H.D., Inc, M.& E., Burton, F., 2003. Wastewater
721 Engineering: Treatment and Reuse. McGraw-Hill Education.
722 Tipping, E., 1981. The adsorption of aquatic humic substances by iron oxides. Geochim.
723 Cosmochim. Acta 45, 191–199. [https://doi.org/10.1016/0016-7037\(81\)90162-9](https://doi.org/10.1016/0016-7037(81)90162-9)

724 Turner, R.C., Miles, K.E., 2011. THE ULTRAVIOLET ABSORPTION SPECTRA OF THE
725 FERRIC ION AND ITS FIRST HYDROLYSIS PRODUCT IN AQUEOUS
726 SOLUTIONS. *Can. J. Chem.* <https://doi.org/10.1139/v57-137>
727 US EPA, O., 2017. Facts and Figures about Materials, Waste and Recycling [WWW Document].
728 US EPA. URL [https://www.epa.gov/facts-and-figures-about-materials-waste-and-](https://www.epa.gov/facts-and-figures-about-materials-waste-and-recycling)
729 [recycling](https://www.epa.gov/facts-and-figures-about-materials-waste-and-recycling) (accessed 12.27.18).
730 Vestin, J.L.K., Norström, S.H., Bylund, D., Lundström, U.S., 2008. Soil solution and stream
731 water chemistry in a forested catchment II: Influence of organic matter. *Geoderma,*
732 *Antarctic Soils and Soil Forming Processes in a Changing Environment* 144, 271–278.
733 <https://doi.org/10.1016/j.geoderma.2007.11.027>
734 Wang, H., Li, F., Keller, A.A., Xu, R., 2009. Chemically enhanced primary treatment (CEPT) for
735 removal of carbon and nutrients from municipal wastewater treatment plants: a case study
736 of Shanghai. *Water Sci. Technol.* 60, 1803–1809. <https://doi.org/10.2166/wst.2009.547>
737 Water Treatability Database [WWW Document], n.d. URL
738 [https://iaspub.epa.gov/tdb/pages/treatment/treatmentOverview.do?processId=19](https://iaspub.epa.gov/tdb/pages/treatment/treatmentOverview.do?processId=1934681921)
739 [34681921](https://iaspub.epa.gov/tdb/pages/treatment/treatmentOverview.do?processId=1934681921) (accessed 9.19.17).
740 Weishaar, J.L., Aiken, G.R., Bergamaschi, B.A., Fram, M.S., Fujii, R., Mopper, K., 2003.
741 Evaluation of Specific Ultraviolet Absorbance as an Indicator of the Chemical
742 Composition and Reactivity of Dissolved Organic Carbon. *Environ. Sci. Technol.* 37,
743 4702–4708. <https://doi.org/10.1021/es030360x>
744 Wilson, A.L., 1959. Determination of fulvic acids in water. *J. Appl. Chem.* 9, 501–510.
745 <https://doi.org/10.1002/jctb.5010091001>
746 Xie, Z., Guan, W., 2015. Research on Fluorescence Spectroscopy Characteristics of Dissolved
747 Organic Matter of Landfill Leachate in the Rear Part of Three Gorges Reservoir [WWW
748 Document]. *J. Spectrosc.* <https://doi.org/10.1155/2015/785406>
749 Zhao, R., Gupta, A., Novak, J.T., Goldsmith, C.D., Driskill, N., 2013a. Characterization and
750 treatment of organic constituents in landfill leachates that influence the UV disinfection
751 in the publicly owned treatment works (POTWs). *J. Hazard. Mater.* 258, 1–9.
752 <https://doi.org/10.1016/j.jhazmat.2013.04.026>
753 Zhao, R., Gupta, A., Novak, J.T., Goldsmith, C.D., Driskill, N., 2013b. Characterization and
754 treatment of organic constituents in landfill leachates that influence the UV disinfection
755 in the publicly owned treatment works (POTWs). *J. Hazard. Mater.* 258–259, 1–9.
756 <https://doi.org/10.1016/j.jhazmat.2013.04.026>
757 Zhou, S., Chen, S., Yuan, Y., Lu, Q., 2015. Influence of Humic Acid Complexation with Metal
758 Ions on Extracellular Electron Transfer Activity. *Sci. Rep.* 5, srep17067.
759 <https://doi.org/10.1038/srep17067>
760